UNH-03-01
LBNL-53972
NT@UW-03-031

Exploring Hyperons and Hypernuclei with Lattice QCD

S.R. Beane,[1,2] P.F. Bedaque,[3] A. Parreño,[4] and M.J. Savage[5]

[1]*Department of Physics, University of New Hampshire, Durham, NH 03824-3568.*
[2]*Jefferson Laboratory, 12000 Jefferson Avenue, Newport News, VA 23606.*
[3]*Lawrence-Berkeley Laboratory, Berkeley, CA 94720.*
[4]*Dept. ECM, Facultat de Física, Universitat de Barcelona, E-08028, Barcelona, Spain.*
[5]*Department of Physics, University of Washington, Seattle, WA 98195-1560.*

Abstract

In this work we outline a program for lattice QCD that would provide a first step toward understanding the strong and weak interactions of strange baryons. The study of hypernuclear physics has provided a significant amount of information regarding the structure and weak decays of light nuclei containing one or two Λ's, and Σ's. From a theoretical standpoint, little is known about the hyperon-nucleon interaction, which is required input for systematic calculations of hypernuclear structure. Furthermore, the long-standing discrepancies in the $P-$wave amplitudes for nonleptonic hyperon decays remain to be understood, and their resolution is central to a better understanding of the weak decays of hypernuclei. We present a framework that utilizes Lüscher's finite-volume techniques in lattice QCD to extract the scattering length and effective range for ΛN scattering in both QCD and partially-quenched QCD. The effective theory describing the nonleptonic decays of hyperons using isospin symmetry alone, appropriate for lattice calculations, is constructed.

I. INTRODUCTION

Nuclear physics is a fascinating field that remains poorly understood at a fundamental level. While the underlying Lagrange density describing all strong interactions is well established to be Quantum Chromo Dynamics (QCD), its solution in the nonperturbative regime leads to many unexpected and intriguing phenomena when the fundamental constants of nature take their physical values. Furthermore, one knows effectively nothing about how most strongly interacting systems behave as the fundamental constants are allowed to move away from their physical values. A puzzling feature of nuclear physics is the unnaturally large size of the $S-$wave nucleon-nucleon scattering lengths; i.e. one would like to understand why low-energy QCD has chosen to be very near an infrared unstable fixed point of the renormalization group, as this requires a non-trivial conspiracy between the quark masses and the scale of QCD, $\Lambda_{\rm QCD}$. While nuclei composed of neutrons and protons are well studied throughout most of the periodic table, and further efforts are proposed to study very short-lived nuclei that impact stellar environments, relatively little is understood about nuclei that contain one or more valence strange quarks: the hypernuclei. Understanding of the structure and decays of hypernuclei from first principles remains at a primitive level, and it is possible that the study of hypernuclei may help in unraveling fundamental issues regarding ordinary nuclei in terms of QCD.

Since the Λ hyperon is the lightest among the hyperons ($m_\Lambda \sim 1115$ MeV), most theoretical and experimental efforts have concentrated on bound systems of non-strange baryons and one Λ. These single-Λ hypernuclei can be experimentally produced by strangeness-exchange reactions $N(K,\pi)\Lambda$ at CERN, BNL, KEK and DaΦne, by strangeness associated production reactions $n(\pi,K)\Lambda$ at BNL and KEK, or by the electroproduction mechanism $p(e,e'K^+\,)\Lambda$ at JLab (also planned at GSI for 2006) [1]. These reactions usually populate highly-excited hypernuclear states, which decay electromagnetically to leave the hyperon in the lowest energy state, $1s_{1/2}$. Once in the ground state, the system decays weakly, without conserving strangeness, parity or isospin. For very-light nuclei, such as ${}^{3}_{\Lambda}$H, the decay proceeds mainly through the mesonic decay mode, $\Lambda \to N\pi$, which is analogous to the decay of the Λ hyperon in free space. These pionic decay channels are highly suppressed when the Λ is embedded in a nuclear medium, as the momentum of the outgoing nucleon (~ 100 MeV) is small compared to the typical Fermi momentum (~ 270 MeV for infinite nuclear matter). Non-mesonic (multi)nucleon induced decay channels, mainly $\Lambda N \to NN$, are then responsible for the decay of the Λ hyperon in the medium, and become dominant for p-shell and heavier systems (note that even for ${}^{5}_{\Lambda}$He, the non-mesonic decay channel amounts to $40\% - 50\%$ of the total decay rate [2]). The lack of stable hyperon beams (the Λ lifetime is $\tau_\Lambda \sim 2.6 \times 10^{-10}$ s) makes it difficult to perform a study of the strong and weak hyperon-nucleon (YN) interaction in free space. Therefore, hypernuclear structure and decay experiments presently provide the only quantitative information on the YN interaction.

Experimental information on hypernuclear decay results from the measure of total lifetimes, partial decay rates (typically from the detection of a proton in the final state, and more recently from the detection of nn and np pairs in coincidence) and angular asymmetry in the emission of protons from the decay of polarized hypernuclei. However, the existing data have large error bars, in part due to poor statistics. On the theoretical side, one has to fold a particular model for the weak $\Lambda N \to NN$ reaction into a many-body system. Realistic ground-state wave functions in the $S = -1$ sector have been derived for $A \leq 4$ hypernuclei using the Faddeev-Yakubovsky formalism [3, 4], and up to $p-$shell

hypernuclei using a three- and four-body cluster structure solved with the Gaussian-basis coupled-rearrangement-channel method [5]. The complete description of the final few-body scattering states in hypernuclear decay has only been performed for $A = 3$ using the Faddeev formalism [3]. For heavier systems, finite nuclei are typically studied within a shell-model framework, while the final state is treated as a distorted wave function describing the two weakly-emitted nucleons moving away from a residual $(A-2)$ core. In any of those calculations, a model for the YN interaction (typically a one-meson-exchange model) is assumed in order to describe the strong two-body dynamics. The development of Effective Field Theories (EFT) in the strong $S = 0$ sector, motivated recent model-independent work in the $S = -1$ sector. An EFT [6] was constructed at next-to-leading order (NLO) for momenta below pion-production threshold, and used to study scattering YN observables, as well as hyperon mass shifts in the medium, via a low-density expansion. The existence of the hypertriton was used to constrain the ΛN singlet- and triplet-scattering lengths. However, a description of bound states using this systematic two-body formalism does not yet exist.

Regarding the $|\Delta S| = 1$ ΛN interaction, all the models developed to date agree in describing the long-range part of the weak transition through the exchange of Goldstone bosons, π, K and η[1]. For the short-range part of the interaction, some studies adopted the exchange of heavier mesons [7, 8], the vector ρ, ω and K^* mesons, while others used a quark-model type description [9]. Although some progress has been achieved during the last ten years, none of the existing models give a satisfactory explanation of the decay process. Construction of a model-independent EFT description of these decays was initiated in Refs. [10, 11]. The study of the $\Delta S = 1$ ΛN interaction has the additional charm of allowing access to both the parity-conserving (PC) and the parity-violating (PV) part of the weak interaction, in contrast to its $\Delta S = 0$ NN partner, where the PC weak signal is masked by the strong PC amplitude which is 10 orders of magnitude larger.

A major tool for strong-interaction physics that will play an ever-increasing role in nuclear physics is lattice QCD. First-principles simulations on the lattice are the only known way to perform rigorous calculations of observables and processes where the QCD strong interaction contributes. Present-day calculations in lattice QCD are restricted to fairly large quark masses, relatively small volumes and relatively large lattice spacings. However, as time progresses the lattice-quark masses are decreasing, lattice sizes are increasing, and lattice spacings are decreasing. Furthermore, it has been appreciated that unphysical simulations performed with partially-quenched QCD (PQQCD) allow for the determination of unquenched QCD observables, and can be performed sooner than fully unquenched simulations. While significant effort has been placed in calculating observables in the meson sector with impressive success, systems involving more than one baryon have largely been ignored with the exception of one pioneering effort to compute the nucleon-nucleon scattering length in quenched QCD [12].

In this work we establish the framework with which lattice (PQ)QCD can determine basic strong-interaction parameters important for hypernuclei: the scattering parameters for $\Lambda N \to \Lambda N$. Given the presently large experimental uncertainties in this scattering amplitude, a lattice calculation will provide an important contribution to refining the potentials that are input into hypernuclear-structure calculations. Another component of this work is to explore the fundamental ingredients of calculations of weak decays of hyperons that

[1] The η-exchange mechanism is omitted in some works due to the smallness (a factor of 10) of the ηNN coupling constants.

must be understood before we are able to claim an understanding of the weak decays of hypernuclei themselves. Such an understanding has eluded theorists for decades; while one appears able to describe the $S-$wave amplitudes in the hyperon nonleptonic weak decays, the $P-$wave amplitudes are very-poorly predicted. Lattice QCD is perhaps the only hope for gaining an understanding of these fundamentally-important weak processes.

II. STRONG ΛN SCATTERING

In predicting the structure of hypernuclei, the hyperon-nucleon potential or the hyperon-nucleon scattering amplitude is required input. A compilation of the world's experimental data on elastic hyperon-nucleon scattering can be found at the Nijmegen "NN-Online" website [13]. The cross-sections in particular energy regions for these processes have large uncertainties associated with them as the total number of events is quite small [2]. To get a sense of the uncertainty in the effective range parameters, consider that Ref. [14] quotes the following one-standard-deviation bounds for the $S-$wave scattering lengths and effective ranges:

$$\begin{aligned} 0.0 \ > \ a^{(^1S_0)} > -15 \text{ fm} \qquad & 0.0 > r^{(^1S_0)} > 15 \text{ fm} \\ -0.6 \ > \ a^{(^3S_1)} > -3.2 \text{ fm} \qquad & 2.5 > r^{(^3S_1)} > 15 \text{ fm} \ . \end{aligned} \tag{1}$$

By comparison, a contemporary study [15] finds (best fit) $a^{(^1S_0)} = -1.8$ fm, $r^{(^1S_0)} = 2.8$ fm, and $a^{(^3S_1)} = -1.8$ fm, $r^{(^3S_1)} = 3.3$ fm. Unfortunately, the meaning of these effective-range analyses is unclear. They arise from a four-parameter fit to data with very-poor statistics at energies where one would not necessarily expect shape parameters and other higher-order terms in the effective-range expansion to be small. Moreover, the effective-range parameters fit to the data are highly correlated. While the bounds of eq. (1) are therefore suspect, they do encompass many model-dependent analyses of hyperfragments, production reactions and potential models [16]. What then is known? Given the current state of experiment, it is probably safe to say: (i) there is no hyperdeuteron and therefore $a^{(^1S_0)} < 0$ and $a^{(^3S_1)} < 0$. (ii) consistency of potential models with the spin of the hypertriton implies $|a^{(^1S_0)}| > |a^{(^3S_1)}|$.

With the lack of experimental effort in the direction of Lambda-nucleon scattering, lattice QCD may provide a rigorous, first-principles calculation of these cross-sections over some energy interval with smaller uncertainties than those determined experimentally in the near (and possibly far) future. In this section we put in place the theoretical framework required to connect possible future lattice calculations with data in the low-energy regime, below the pion-production threshold.

The past decade has seen remarkable progress in the development of an EFT description of nucleon-nucleon (NN) scattering. Two quite different power-countings were developed for these processes, Weinberg [17, 18, 19, 20] and KSW power-counting [21, 22, 23, 24], with neither providing a complete description of scattering in all partial waves. A third power-counting, BBSvK counting [25], which is essentially a synthesis of these countings appears to be both formally consistent and provides a convergent expansion. The difficulty in establishing an EFT description is due to the large scattering lengths in both the $^1S_0$ and $^3S_1$ channels, or equivalently, the near threshold (un)bound states in both channels.

[2] We are grateful to Rob Timmermans for discussions about the state of hyperon-nucleon scattering data.

Such states cannot be generated at any order in perturbation theory, and require the non-perturbative resummation of at least one operator in the theory. Physically speaking, such states result from a fine-tuning between kinetic and potential energy, and imply that the EFT is in the proximity of an unstable infrared fixed point [26] (and thus implies that QCD has an infrared unstable fixed point).

There is no reason to suppose that the hyperon-nucleon sector is near an infrared fixed point. That is to say, while the bounds of eq. (1) do not preclude unnaturally large scattering lengths, we would expect the scattering lengths to be of natural size, and for there to be no ΛN bound states near threshold. Therefore, one expects the EFT that describes the interaction between hyperons and nucleons to have a power-counting based on the engineering dimensions of the operators that appear in the effective Lagrange density, and hence to be precisely the power-counting of Weinberg [17, 18] [3]. As a well-defined procedure exists, due to Lüscher [27, 28], for extracting the low-energy elastic scattering parameters from finite-volume lattice QCD calculations, we set-up the low-energy EFT describing ΛN scattering in Weinberg power-counting[4]. Given the Lüscher framework, we use the EFT to compute the scattering length and effective range for elastic ΛN scattering to NLO in the EFT expansion [5]. These parameters will be sufficient to describe ΛN scattering for energies below that necessary for inelastic processes $\Lambda N \to \Sigma N$ and $\Lambda N \to \Lambda N \pi$. (See also Ref. [6].) Our results contain the leading light-quark mass dependence of low-energy ΛN scattering and can be used to extrapolate from lattice-quark mass values to nature.

A. $\Lambda N \to \Lambda N$ in QCD

If one could perform a lattice QCD simulation at the physical values of the quark masses, then, barring the advent of new experiments, there would be no need to construct the EFT for the $\Lambda N \to \Lambda N$ S-matrix at low energies. However, near-future lattice simulations will be partially-quenched with unphysically large values of the sea-quark masses. Therefore, at least in the short term, the EFT construction will be needed to extrapolate to QCD.

In defining the nonrelativistic fields appropriate for computing the strong interactions between the Λ and the nucleon we remove the nucleon classical trajectory from the nucleon field, and the Λ classical trajectory from the Λ field [6]. We can perform these redefinitions as we will work with an $SU(2)_L \otimes SU(2)_R$ chirally-invariant theory, as opposed to its three-flavor analog. The Lagrange density describing the free-field dynamics of the nucleon, Λ and Σ is

$$\mathcal{L} \;=\; N^\dagger \left(i\partial_0 + \frac{\nabla^2}{2M_N} \right) N \;+\; \Lambda^\dagger \left(i\partial_0 + \frac{\nabla^2}{2M_\Lambda} \right) \Lambda \;+\; \Sigma^\dagger \;\left(i\partial_0 + \frac{\nabla^2}{2M_\Lambda} - \Delta_{\Sigma\Lambda} \right) \Sigma \quad , \quad (2)$$

[3] Weinberg's power-counting does not, in general, *require* resummation of interactions.

[4] Note, however, that we power-count the amplitude directly, rather than the potential.

[5] The three-body system with one Λ-hyperon has been investigated in an EFT without pions [29].

[6] Usually, one removes only the classical trajectory associated with one of the heavy-hadron fields. However, we will work with two-flavor χPT in which strange-baryon number is conserved at each interaction, and hence the ΛN residual mass term, $\Delta_{\Lambda N}$ can be removed from the theory by a phase redefinition, leaving only the $\Sigma\Lambda$ residual mass term.

where Λ is an iso-singlet while the nucleon iso-doublet and the Σ iso-triplet are defined as

$$N \;=\; \begin{pmatrix} p \\ n \end{pmatrix} \quad , \quad \Sigma \;=\; \begin{pmatrix} \Sigma^0/\sqrt{2} & \Sigma^+ \\ \Sigma^- & -\Sigma^0/\sqrt{2} \end{pmatrix} \quad . \tag{3}$$

As we are interested only in ΛN scattering up to NLO, we need not consider the Weinberg-Tomazawa type interactions. The complete kinetic energy terms for the N and Σ have additional multi-pion interactions, but as the Λ is an isosinglet its chirally-invariant kinetic energy term is given in eq. (2). The leading-order (LO) interactions between the baryons and the pions are given by (to linear order in the pion field)

$$\begin{aligned} \mathcal{L} \;=\; & \frac{g_A}{f}\, N^\dagger \sigma\cdot\nabla M N \;+\; \frac{g_{\Lambda\Sigma}}{f}\, \Big(\Lambda^\dagger \mathrm{Tr}\big[\, \sigma\cdot\nabla M \Sigma \,\big] \;+\; \mathrm{h.c.}\Big) \\ & + \frac{g_{\Sigma\Sigma}}{f}\, \mathrm{Tr}\Big[\, \Sigma^\dagger \left[\sigma\cdot\nabla M \;,\; \Sigma\,\right]\Big] \quad , \end{aligned} \tag{4}$$

where $f \sim 132$ MeV is the pion decay constant, $g_A \sim 1.27$ is the nucleon axial coupling constant, $g_{\Lambda\Sigma} \sim 0.60$ is the $\Lambda\Sigma$ axial coupling constant, while $g_{\Sigma\Sigma}$ is the $\Sigma\Sigma$ axial coupling that cannot be determined directly from experiment and which we will discuss later. M is the matrix of pions given by

$$M \;=\; \begin{pmatrix} \pi^0/\sqrt{2} & \pi^+ \\ \pi^- & -\pi^0/\sqrt{2} \end{pmatrix} \quad . \tag{5}$$

At LO in the expansion, there will be contributions to $S-$wave scattering from four-baryon operators of the form

$$\mathcal{L} \;=\; {}_{\Lambda\Lambda}C_0^{(^1S_0)} \Big(\Lambda^T\, P^{(^1S_0)}\, N\Big)^\dagger \Big(\Lambda^T\, P^{(^1S_0)}\, N\Big) + \; {}_{\Lambda\Lambda}C_0^{(^3S_1)} \Big(\Lambda^T\, P^{(^3S_1)}\, N\Big)^\dagger \Big(\Lambda^T\, P^{(^3S_1)}\, N\Big) \tag{6}$$

where $P^{(^1S_0)} = \frac{1}{\sqrt{2}}\, i\sigma_2$ and $P^{(^3S_1)} = \frac{1}{\sqrt{2}}\, i\sigma_2\sigma^a$ are spin-projectors for the ${}^1S_0$ and ${}^3S_1$ channels respectively, and the coefficients ${}_{\Lambda\Lambda}C_0^{(^1S_0,{}^3S_1)}$ are to be determined. At next-to-leading order (NLO) there are also contributions from four-baryon operators that involve a Σ baryon,

$$\begin{aligned} \mathcal{L} \;=\; & {}_{\Sigma\Lambda}C_0^{(^1S_0)} \Big(\Sigma^T (i\tau_2)\, P^{(^1S_0)}\, N\Big)^\dagger \Big(\Lambda^T (i\tau_2)\, P^{(^1S_0)}\, N\Big) \\ & + \; {}_{\Sigma\Lambda}C_0^{(^3S_1)} \Big(\Sigma^T (i\tau_2)\, P^{(^3S_1)}\, N\Big)^\dagger \Big(\Lambda^T (i\tau_2)\, P^{(^3S_1)}\, N\Big) \;+\; \mathrm{h.c.} \quad , \end{aligned} \tag{7}$$

where the coefficients ${}_{\Sigma\Lambda}C_0^{(^1S_0,{}^3S_1)}$ are to be determined.

We have recognized and implemented a particular hierarchy of mass-scales in order to simplify our expressions for the scattering length and effective range. By returning briefly to $SU(3)$, we recall that the $\Sigma\Lambda$ mass splitting, $\Delta_{\Lambda\Sigma} \sim m_q$ is proportional to the light-quark masses, in particular, the strange quark mass, and numerically is $\Delta_{\Lambda\Sigma} \sim 74$ MeV. In contrast, the pion mass is $m_\pi \sim m_q^{1/2}$ and numerically is $m_\pi \sim 140$ MeV. Therefore, in what follows we will neglect $\Delta_{\Lambda\Sigma}$ compared to m_π. However, we will retain terms of the form $\sqrt{2\mu_{\Lambda N}\Delta_{\Lambda\Sigma}}$ (where $\mu_{\Lambda N}$ is the reduced mass of the ΛN system) compared to m_π, as they are of the same order in the $SU(3)$ chiral expansion. While we can (somewhat) justify this expansion from a formal point of view, one should keep in mind that the expansion is in factors of ~ 2. Of course the sole purpose of this expansion is to provide simple closed-form expressions for the effective-range parameters; the exact numerical expressions are easily obtained and may in fact be necessary in certain regions of the C_0 parameter space.

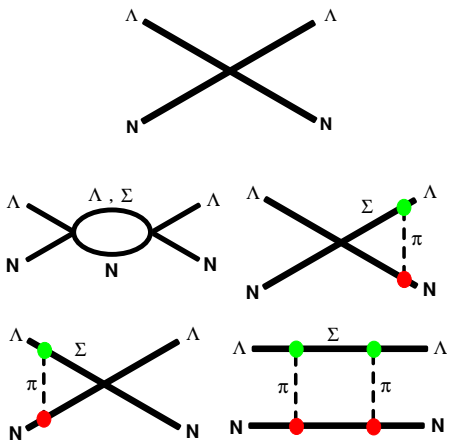

FIG. 1: *Diagrams that contribute to ΛN scattering at LO (top) and NLO in the EFT. The shaded blobs are vertices from eq. (4).*

A straightforward calculation of the diagrams in Fig. 1 yields the scattering length $a^{(^1S_0)}$ and effective range $r^{(^1S_0)}$ in the $^1S_0$ channel:

$$\begin{aligned} a^{(^1S_0)} &= -\frac{\mu_{\Lambda N}}{2\pi}\left[{}_{\Lambda\Lambda}C_0^{(^1S_0)} - \frac{3}{4\pi}\left({}_{\Sigma\Lambda}C_0^{(^1S_0)}\right)^2 \mu_{\Lambda N}\,\eta + {}_{\Sigma\Lambda}C_0^{(^1S_0)}\,\frac{3g_{\Sigma\Lambda}\,g_A\,\mu_{\Lambda N}}{2\pi f^2}\,\frac{\eta^2+\eta m_\pi+m_\pi^2}{\eta+m_\pi}\right. \\ &\quad \left. - \frac{3g_{\Sigma\Lambda}^2\,g_A^2\,\mu_{\Lambda N}}{4\pi f^4}\,\frac{2\eta^3+4\eta^2 m_\pi+6\eta m_\pi^2+3m_\pi^3}{2(\eta+m_\pi)^2}\right]; \\ r^{(^1S_0)} &= -\frac{1}{\mu_{\Lambda N}\,\pi}\left[\frac{2\pi}{{}_{\Lambda\Lambda}C_0^{(^1S_0)}}\right]^2\left[\frac{3}{8\pi}\left({}_{\Sigma\Lambda}C_0^{(^1S_0)}\right)^2\frac{\mu_{\Lambda N}}{\eta} - {}_{\Sigma\Lambda}C_0^{(^1S_0)}\,\frac{3g_{\Sigma\Lambda}\,g_A\,\mu_{\Lambda N}}{2\pi f^2}\,\frac{3\eta^2+9\eta m_\pi+8m_\pi^2}{6(\eta+m_\pi)^3}\right. \\ &\quad \left. + \frac{3g_{\Sigma\Lambda}^2\,g_A^2\,\mu_{\Lambda N}}{4\pi f^4}\,\frac{6\eta^3+23\eta^2 m_\pi+28\eta m_\pi^2+7m_\pi^3}{12(\eta+m_\pi)^4}\right], \end{aligned} \tag{8}$$

where $\eta=\sqrt{2\mu_{\Lambda N}\Delta_{\Lambda\Sigma}}$. We see that there are two unknown constants, ${}_{\Lambda\Lambda}C_0^{(^1S_0)}$ and ${}_{\Sigma\Lambda}C_0^{(^1S_0)}$, and two observables, $a^{(^1S_0)}$ and $r^{(^1S_0)}$. In the spin-triplet channel we find

$$\begin{aligned} a^{(^3S_1)} &= -\frac{\mu_{\Lambda N}}{2\pi}\left[{}_{\Lambda\Lambda}C_0^{(^3S_1)} - \frac{3}{4\pi}\left({}_{\Sigma\Lambda}C_0^{(^3S_1)}\right)^2 \mu_{\Lambda N}\,\eta - {}_{\Sigma\Lambda}C_0^{(^3S_1)}\,\frac{g_{\Sigma\Lambda}\,g_A\,\mu_{\Lambda N}}{2\pi f^2}\,\frac{\eta^2+\eta m_\pi+m_\pi^2}{\eta+m_\pi}\right. \\ &\quad \left. - \frac{3g_{\Sigma\Lambda}^2\,g_A^2\,\mu_{\Lambda N}}{4\pi f^4}\,\frac{2\eta^3+4\eta^2 m_\pi+6\eta m_\pi^2+3m_\pi^3}{2(\eta+m_\pi)^2}\right], \end{aligned} \tag{9}$$

and

$$\begin{aligned} r^{(^3S_1)} &= -\frac{1}{\mu_{\Lambda N}\pi}\left[\frac{2\pi}{{}_{\Lambda\Lambda}C_0^{(^3S_1)}}\right]^2\left[\frac{3}{8\pi}\left({}_{\Sigma\Lambda}C_0^{(^3S_1)}\right)^2\frac{\mu_{\Lambda N}}{\eta} + {}_{\Sigma\Lambda}C_0^{(^3S_1)}\,\frac{g_{\Sigma\Lambda}\,g_A\,\mu_{\Lambda N}}{2\pi f^2}\,\frac{3\eta^2+9\eta m_\pi+8m_\pi^2}{6(\eta+m_\pi)^3}\right. \\ &\quad \left. - \frac{3g_{\Sigma\Lambda}^2\,g_A^2\,\mu_{\Lambda N}}{4\pi f^4}\,\frac{46\eta^3+91\eta^2 m_\pi+44\eta m_\pi^2+11m_\pi^3}{36(\eta+m_\pi)^4}\right], \end{aligned} \tag{10}$$

where we again see that there are two unknown constants, ${}_{\Lambda\Lambda}C_0^{(^3S_1)}$ and ${}_{\Sigma\Lambda}C_0^{(^3S_1)}$, and two observables, $a^{(^3S_1)}$ and $r^{(^3S_1)}$.

It is worth commenting on the viability of the power-counting scheme that we have chosen for the ΛN system. Consider the ${}^1S_0$ effective-range parameters of eq. (8). If we vary the $C_0^{({}^1S_0)}$ coefficients over natural values (i.e. $\sim 1/f^2$), then there are large regions of parameter space where there is poor convergence in the scattering length, and the effective range is anomalously small and negative. This may indicate that a next-to-NLO (NNLO) calculation is required, which includes, *inter alia*, contact operators with two derivatives (the C_2 operators) and contact operators with an insertion of the quark-mass matrix (the D_2 operators). However, it may also be the case that we should apply our power-counting scheme to a potential, rather than the amplitude directly, and resum using the Schrödinger equation, as in Weinberg power-counting in the NN system. The appropriate power-counting will ultimately have to be decided in conjunction with lattice QCD simulations of the ΛN system.

B. $\Lambda N \to \Lambda N$ in PQQCD

While one always hopes for fully-unquenched lattice simulations at the physical values of the light-quark masses, it will always be the case that partially-quenched simulations of the observables of interest will be performed first. This is for the simple reason that the partially-quenched simulations, in which the masses of the sea-quarks are larger than those of the valence quarks, take less time than the fully-unquenched simulations. During the past year or so a significant number of single-nucleon observables have been explored in partially-quenched chiral perturbation theory (PQχPT) [30, 31, 32] with an eye to making connections between partially-quenched lattice simulations and nature. The EFT describing NN interactions has also been partially quenched [33, 34].

The partial quenching of the ΛN scattering amplitude has features from both the partially-quenched NN scattering amplitude [34] and from the $\Lambda_Q\Lambda_Q$ potential [35]. The local four-baryon operators in PQQCD are the same as those in QCD because ghost-quark and sea-quark number are conserved. It is for this reason that the pion box-diagram is the same in PQQCD and QCD. The Crossed-Box diagram is modified by partial quenching, but this effect enters at NNLO, one order beyond the order to which we are working. Unlike the $\Lambda_Q\Lambda_Q$ potential [35], there is a contribution from one-hairpin exchange (OHPE) at LO and also from one- and two-hairpin exchanges at NLO, as shown in Fig. 2.

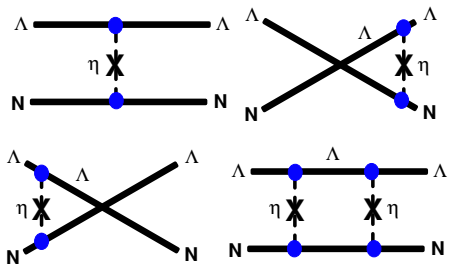

FIG. 2: *The LO and NLO contributions to ΛN scattering from hairpin-exchange in PQχPT. The shaded blobs are vertices from eq. (12).*

The $SU(2)_L \otimes SU(2)_R$ chiral symmetry of two-flavor QCD is extended to the graded

$SU(4|2)_L \otimes SU(4|2)_R$ chiral symmetry of PQQCD, as discussed extensively in Refs. [31, 32]. In this theory, in addition to the light pions, light ghost-mesons and sea-mesons that contribute in diagrams with single-pole propagators, there are also contributions from η-exchange with a double-pole propagator of the form

$$G_{\eta\eta}(q^2) \;=\; \frac{i(m_{ss}^2 - m_\pi^2)}{(q^2 - m_\pi^2 + i\epsilon)^2} \quad , \tag{11}$$

where m_{ss} is the mass of a meson composed only of sea quarks. We are working in the isospin limit where the sea-quarks are degenerate and the valence quarks are degenerate. This double-pole arises because the singlet of $SU(2)$ is not the singlet of $SU(4|2)$ [39]. At LO in the chiral expansion, the interaction between the η and the baryons is described by a Lagrange density of the form

$$\mathcal{L} \;=\; \frac{1}{\sqrt{2}f}\; g_0^{(N)}\; N^\dagger \sigma^k N\; \nabla^k \eta \;+\; \frac{1}{\sqrt{2}f} g_0^{(\Lambda)}\; \Lambda^\dagger \sigma^k \Lambda \nabla^k \eta \quad , \tag{12}$$

where the axial couplings, $g_0^{(N,\Lambda)}$ are to be determined from lattice simulations. The analogous contributions to the $\Lambda_Q\Lambda_Q$ potential [35] are absent because the axial coupling of the hairpin to the Λ_Q vanishes due to heavy-quark symmetry, and is non-zero only at order $1/m_Q$ [36]. However, we expect the coupling $g_0^{(\Lambda)}$ to be significantly smaller than $g_{\Sigma\Lambda}$ based on large-N_C arguments. In the large-N_C limit, the "size" of the matrix element of an operator with isospin I and spin J is of order $1/N_C^{|I-J|}$ [37, 38]. Hence we expect this axial coupling, which has $I = 0$ and $J = 1$, to be suppressed by a factor of ~ 3 compared to $g_{\Sigma\Lambda}$, which gives it a natural size of $g_0^{(\Lambda)} \sim 0.2$.

We find that the leading contributions to the scattering length and effective range in the ${}^1S_0$ channel due to partial quenching are

$$\begin{aligned}
\delta a^{({}^1S_0)} \;&=\; -\frac{\mu_{\Lambda N}}{2\pi}\left[{}_{\Lambda\Lambda}C_0^{({}^1S_0)} \frac{g_0^{(\Lambda)} g_0^{(N)} \mu_{\Lambda N}}{4\pi f^2} \frac{m_{ss}^2 - m_\pi^2}{m_\pi} \;+\; \frac{(g_0^{(\Lambda)})^2 (g_0^{(N)})^2 \mu_{\Lambda N}}{128\pi f^4} \frac{(m_{ss}^2 - m_\pi^2)^2}{m_\pi^3} \right] ; \\
\delta r^{({}^1S_0)} \;&=\; -\frac{1}{\mu_{\Lambda N}\pi}\left[\frac{2\pi}{{}_{\Lambda\Lambda}C_0^{({}^1S_0)}} \right]^2 \frac{g_0^{(\Lambda)} g_0^{(N)}}{f^2} \frac{m_{ss}^2 - m_\pi^2}{m_\pi^4} \quad ,
\end{aligned} \tag{13}$$

and in the ${}^3S_1$ channel are

$$\begin{aligned}
\delta a^{({}^3S_1)} \;&=\; -\frac{\mu_{\Lambda N}}{2\pi}\left[-{}_{\Lambda\Lambda}C_0^{({}^3S_1)} \frac{g_0^{(\Lambda)} g_0^{(N)} \mu_{\Lambda N}}{12\pi f^2} \frac{m_{ss}^2 - m_\pi^2}{m_\pi} \;+\; \frac{(g_0^{(\Lambda)})^2 (g_0^{(N)})^2 \mu_{\Lambda N}}{128\pi f^4} \frac{(m_{ss}^2 - m_\pi^2)^2}{m_\pi^3} \right] ; \\
\delta r^{({}^3S_1)} \;&=\; +\frac{1}{\mu_{\Lambda N}\pi}\left[\frac{2\pi}{{}_{\Lambda\Lambda}C_0^{({}^3S_1)}} \right]^2 \frac{g_0^{(\Lambda)} g_0^{(N)}}{3f^2} \frac{m_{ss}^2 - m_\pi^2}{m_\pi^4} \quad .
\end{aligned} \tag{14}$$

It is important to note that the additional contributions to the scattering lengths arise from the NLO diagrams in Fig. 2, and as required, there is no contribution from OHPE (due to the derivative coupling). By contrast, the contribution to the effective ranges begins at LO from OHPE. Therefore, partial-quenching will perturbatively modify the scattering lengths, but overwhelmingly dominate the effective ranges, except very near the QCD limit. Given that extractions of both the scattering length and effective range are required to determine the four-baryon, momentum-independent leading-order interactions, partial-quenching may provide a serious obstacle to this procedure.

C. $\Lambda N \to \Lambda N$ at Finite Volume

The Maiani-Testa theorem [40] precludes determination of scattering amplitudes from Euclidean-space Green functions at infinite volume away from kinematic thresholds. While appearing to be a significant setback for lattice QCD for which only Euclidean-space Green functions can be computed, it was realized by Lüscher [27, 28] that one can access $2 \to 2$ scattering amplitudes from lattice calculations performed at finite volume. Lüscher's work generalizes a result from nonrelativistic quantum mechanics [41] to quantum field theory. The results are obtained by assuming that the lattice spacing, b [7], is very small and the lattice size, L, is much larger than the range of the potential between the two particles.

During the past few years, the pionless effective field theory, EFT($\not\pi$) [42, 43], description of NN scattering at momenta much less than the pion mass has been studied extensively, and it can be applied to describe the finite-volume construction described above [8]. In EFT($\not\pi$) the interactions between nucleons are described by a series of delta-functions and their derivatives. While the two-nucleon sector reproduces identically effective-range theory, when gauge fields are included one has a systematic and calculable scheme with which to determine all low-energy multi-nucleon processes. This theory has been successfully applied to quite a wide variety of two-nucleon and three-nucleon processes[9]. In order to establish a power-counting at the level of diagrams in systems with unnaturally-large scattering lengths, the power-divergence subtraction scheme (PDS) was introduced to deal with the power-law ultra-violet divergences that appear in the non-relativistic theory at the one-loop level. It is somewhat useful to see how one recovers Lüscher's relations between the energy-levels of the quantum system in a periodic box and the scattering parameters of the continuum theory in EFT($\not\pi$), and this is presented in Appendix I. As re-derived in Appendix I, the energy of the lowest-lying scattering state of the two-particle system with zero center of mass momentum in a periodic box of sides L that is much greater than any of the scattering parameters, such as the scattering length and effective range, is [27, 28]

$$E_0 \;=\; +\frac{2\pi a}{\mu_{\Lambda N}\; L^3}\left[\; 1 \;-\; c_1\frac{a}{L} \;+\; c_2\left(\frac{a}{L}\right)^2 \;+\; ...\right] \;+\; \mathcal{O}(L^{-6}) \quad , \tag{15}$$

where the coefficients $c_{1,2}$ are $c_1 = -2.837297$ and $c_2 = 6.375183$, and where we have used the conventional definition of scattering length and effective range

$$p\cot\delta \;=\; -\frac{1}{a} + \frac{1}{2}rp^2 + ... \quad . \tag{16}$$

The energy of the next level which transforms in the A_1 representation of the cubic group

[7] In this work we use b instead of a to denote the lattice spacing. Clearly this will be considered a sacrilege in the lattice community, but denoting the lattice spacing by the traditional a would lead to confusion with the scattering lengths which are also traditionally denoted by a.

[8] This discussion will be the same as that for pseudo-potentials [44] as the "physics" is the same. However the EFT($\not\pi$) construction allows for generalization to processes including gauge fields.

[9] One may worry about potential violations of unitarity in EFT($\not\pi$) for PQQCD. However, as pointed out in Ref. [34], one can use the methods of Ref. [33] to show that all effects of partial-quenching are in the coefficients of the contact operators. Therefore, perhaps somewhat surprisingly, EFT($\not\pi$) is unitary in PQQCD.

is [27, 28]

$$E_1 \;=\; \frac{2\pi^2}{\mu_{\Lambda N}\; L^2} - \frac{6\tan\delta_0}{\mu_{\Lambda N}\; L^2}\Big(\; 1 + c_1'\tan\delta_0 + c_2'\tan^2\delta_0 \;+\; ...\;\Big) \;+\; \mathcal{O}(L^{-6}) \quad , \qquad (17)$$

where $c_1' = -0.061367$ and $c_2' = -0.354156$, and where δ_0 is the $S-$wave phase shift evaluated at the unperturbed lattice momentum $|\mathbf{p}| = 2\pi/L$. It is important to stress that the effective-range parameters may be comparable to or greater than realistic box sizes at some values of the unphysical lattice quark masses. Eqs. (15) and (17) are then no longer applicable and one must use the exact formula for the energy levels, eq. (38), given in Appendix I.

III. NONLEPTONIC WEAK DECAYS AND WEAK HYPERNUCLEAR DECAYS

The weak decays of hypernuclei result not only from the one-body nonleptonic decays (mesonic) of the hyperon(s), e.g. $\Lambda \to N\pi$, that exists in free-space but also from two- and higher-body decays (non-mesonic), such as $\Lambda N \to NN$ and $\Lambda NN \to NNN$. Naive expectations suggest that the one-body decays should dominate, however the non-mesonic processes are found to be comparable to the mesonic decays in nuclei, in part due to Pauli-blocking of the final-state nucleon in mesonic decays.

The nonleptonic weak decays of hyperons in free-space have been very-well studied during the past many decades. While the $S-$ and $P-$wave amplitudes that contribute to each process are very-well known experimentally, the $P-$wave amplitudes are still not well described theoretically. In order for one to claim that the weak decays of hypernuclei are theoretically understood we must first understand the nonleptonic weak decays of hyperons in free-space, as this underlies one of the two competing decay processes. Furthermore, the EFT that describes these processes is more than likely entangled in the theory that describes the higher-body amplitudes, and therefore is central to the description of all decay processes.

A. Nonleptonic Weak Decays of Hyperons in Free-Space

As the nonleptonic decays $\Lambda \to p\pi^-$, $\Sigma^- \to n\pi^-$, $\Sigma^+ \to n\pi^+$, $\Xi^- \to \Lambda\pi^-$ and their isospin partners have been well studied for an extensive period of time, the experimental data and theoretical efforts to understand the data can be found in many textbooks, e.g. Ref. [45]. Therefore, we do not attempt an exhaustive discussion of the existing literature in this work. Angular-momentum considerations are sufficient to write the matrix element for the nonleptonic decay $B \to B'\pi$, $\mathcal{M}_{BB'\pi}$, using the notation of Jenkins [46], as

$$\mathcal{M} \;=\; G_F m_{\pi^+}^2\; \overline{U}_{B'}\; \Big[\mathcal{A}^{(S)} \;+\; 2\; S^\mu \hat{k}_\mu\; \mathcal{A}^{(P)}\Big]\; U_B \quad , \qquad (18)$$

where $\hat{k}$ is the four-vector of the outgoing pion normalized to the pion three-momentum in the baryon rest frame. The factor of $m_{\pi^+}^2$ that appears in the coefficient in eq. (18) is the physical mass of the charged pion, and does not indicate that the amplitude vanishes in the chiral limit. The amplitudes $\mathcal{A}^{(S)}$ and $\mathcal{A}^{(P)}$ are the $S-$ and $P-$wave amplitudes, respectively. They are expected to be the same order in the chiral expansion, and indeed experimentally, their magnitudes are of order unity.

1. *Nonleptonic Weak Decays of Hyperons in SU(3)*

Conventionally, the theoretical analysis of these decays is performed about the limit of $SU(3)$ flavor symmetry, assuming the $\Delta I = \frac{1}{2}$ rule, although a more general analysis shows that the $\Delta I = \frac{1}{2}$ rule is well respected in these decays [45]. At LO in the chiral expansion, the weak decays are described by the Lagrange density

$$\mathcal{L} \;=\; G_F \; m_{\pi^+}^2 \; f \;\left(\; h_D \;\mathrm{Tr}\left[\overline{B}\{h_\xi, B\}\right] \;+\; h_F \;\mathrm{Tr}\left[\overline{B}\,[h_\xi, B]\right]\;\right) \quad , \tag{19}$$

where

$$h_\xi \;=\; \xi^\dagger \; h \; \xi \quad \text{with} \quad h \;=\; \begin{pmatrix} 0 & 0 & 0 \\ 0 & 0 & 1 \\ 0 & 0 & 0 \end{pmatrix} \quad , \tag{20}$$

and where h transforms as a $(\mathbf{8}, \mathbf{1})$, $h \to L h L^\dagger$, under $SU(3)_L \otimes SU(3)_R$ chiral transformations. Expanding this interaction to linear order in the pion field, it is straightforward to show that the $S-$amplitudes arising from the diagram in Fig. 3 or its analog are [46, 47]

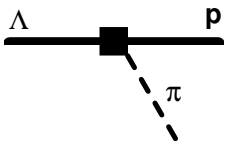

FIG. 3: *Tree-level diagram that gives the leading-order contribution to the $S-$wave amplitudes for the nonleptonic decay $\Lambda \to p\pi^-$. The solid square denotes an insertion of the leading-order weak interaction from eq. (19).*

$$\begin{array}{llll} \mathcal{A}^{(S)}_{\Lambda p\pi^-} \;=\; -\frac{1}{\sqrt{6}}\,(h_D + 3h_F) & & \mathcal{A}^{(S)}_{\Sigma^- n\pi^-} \;=\; h_D - h_F \\ \mathcal{A}^{(S)}_{\Sigma^+ n\pi^+} \;=\; 0 & & \mathcal{A}^{(S)}_{\Xi^-\Lambda\pi^-} \;=\; \frac{1}{\sqrt{6}}\,(3h_F - h_D) \end{array} \tag{21}$$

and the $P-$wave amplitudes arising from the diagrams in Fig. 4 and their analogs are

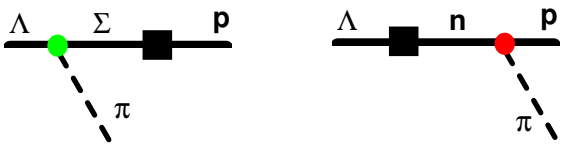

FIG. 4: *Tree-level diagrams that give the leading-order contribution to the $P-$wave amplitudes for the nonleptonic decay $\Lambda \to p\pi^-$. The solid-square denotes an insertion of the leading-order weak interaction from eq. (19) while the shaded circles denote axial couplings.*

$$
\begin{aligned}
\mathcal{A}^{(P)}_{\Lambda p\pi^-} &= \frac{\sqrt{\frac{2}{3}}D(h_D-h_F)}{M_p-M_{\Sigma^+}} - \frac{(D+F)(h_D+3h_F)}{\sqrt{6}(M_\Lambda-M_n)} \\
\mathcal{A}^{(P)}_{\Sigma^- n\pi^-} &= \frac{F(h_F-h_D)}{M_n-M_{\Sigma^0}} - \frac{D(h_D+3h_F)}{3(M_n-M_\Lambda)} \\
\mathcal{A}^{(P)}_{\Sigma^+ n\pi^+} &= -\frac{D(h_D+3h_F)}{3(M_n-M_\Lambda)} - \frac{F(h_F-h_D)}{M_n-M_{\Sigma^0}} + \frac{(D+F)(h_D-h_F)}{M_{\Sigma^+}-M_p} \\
\mathcal{A}^{(S)}_{\Xi^-\to\Lambda\pi^-} &= \frac{(D-F)(3h_F-h_D)}{\sqrt{6}(M_\Lambda-M_{\Xi^0})} + \sqrt{\frac{2}{3}}\frac{D(h_D+h_F)}{M_{\Xi^-}-M_{\Sigma^-}} \quad ,
\end{aligned} \tag{22}
$$

where D and F describe the matrix elements of the octet axial current operators between octet baryons.

In table I we present the numerical values for the LO tree-level amplitudes, along with their experimental values. We choose to determine h_D and h_F from the $S-$wave amplitudes, which give central values $h_D = 0.58$ and $h_F = -1.40$, and to use the tree-level values for the axial matrix elements, $D = 0.80$ and $F = 0.50$ [10]. Also, in table I we present the amplitudes

TABLE I: Weak Amplitudes in $SU(3)$ χPT at LO and NLO

Decay	$\mathcal{A}^{(S)}$ LO	$\mathcal{A}^{(S)}$ NLO [50]	$\mathcal{A}^{(S)}$ Expt	$\mathcal{A}^{(P)}$ LO	$\mathcal{A}^{(P)}$ NLO [50]	$\mathcal{A}^{(P)}$ Expt
$\Lambda \to p\pi^-$	1.48	1.44	1.42 ± 0.01	0.59	-0.73 ± 0.18	0.52 ± 0.02
$\Sigma^- \to n\pi^-$	1.98	1.89	1.88 ± 0.01	-0.30	0.46 ± 0.21	-0.06 ± 0.01
$\Sigma^+ \to n\pi^+$	0.0	0.01	0.06 ± 0.01	0.16	-0.18 ± 0.21	1.81 ± 0.01
$\Xi^- \to \Lambda\pi^-$	-1.95	-2.01	-1.98 ± 0.01	-0.19	0.52 ± 0.29	0.48 ± 0.02

that are found at one-loop order (NLO) in the three-flavor chiral expansion [50] (see also Ref. [51]).

The numerical values in table I make it clear that the theoretical analysis does not come close to predicting the $P-$wave amplitudes. Moreover, the one-loop computation in three-flavor χPT [47, 49, 50, 51] does not improve the situation and, arguably, makes the situation worse. There are a variety of reasons one can conjecture as a possible explanation of these discrepancies, e.g. $SU(3)$ breaking is abnormally large, there are strong final state interactions, there are narrow hadronic resonances (e.g. pentaquarks) in some channels, and so forth. From a formal standpoint, it is possible that the three-flavor χPT expansion simply does not behave well for these observables, given that it is the kaon mass that is governing the convergence. Jenkins [46] has argued that convergence is poor, not due to failure of the chiral expansion, but due to large cancellations at LO. In order to explore this possibility further, a NNLO calculation is ultimately required. As parameters that enter into the NLO calculations were determined from a global fit it is somewhat difficult to determine if the problems in the $P-$waves lie in only one of the decay modes or if the theory fails equally badly in all modes.

[10] Ref. [48] finds $D = 0.79 \pm 0.10$ and $F = 0.47 \pm 0.07$ from a global fit of tree-level axial matrix elements to the available semileptonic decay data.

2. Nonleptonic Weak Decays of Hyperons in $SU(2)$

Given the absence of complete theoretical control in the nonleptonic decays in three-flavor χPT, we de-scope our efforts to two-flavor χPT with the hope of gaining some insight into which processes can be identified as problematic and which are under control, without having to consider the issue of $SU(3)$ breaking. We restrict ourselves to the decays of the Λ and Σ as we are primarily interested in the study of hypernuclei containing these hyperons.

At LO in the two-flavor chiral expansion, the weak Lagrange density is

$$\mathcal{L} \;=\; G_F m_{\pi^+}^2 f \left[\; h_\Lambda \;\left(\overline{N} h_\xi\right) \Lambda \;+\; h_\Sigma \;\overline{N} \Sigma h_\xi \;+\; \text{h.c.} \;\right] \quad , \tag{23}$$

where

$$h_\xi \;=\; \xi^\dagger h \;\text{ and }\; h \;=\; \begin{pmatrix} 0 \\ 1 \end{pmatrix} \quad , \tag{24}$$

and where h, which transforms as $h \to Lh$ under $SU(2)_L \otimes SU(2)_R$ chiral transformations, is a $(\mathbf{2},\mathbf{1})$. As in the three-flavor case, we have assumed a $\Delta I = \frac{1}{2}$ weak interaction only.

The weak interactions described in eq. (23) along with the strong interactions between the pions and the baryons in eq. (4) give $S-$wave amplitudes

$$\mathcal{A}^{(S)}_{\Lambda p\pi^-} \;=\; h_\Lambda \quad , \; \mathcal{A}^{(S)}_{\Sigma^- n\pi^-} \;=\; h_\Sigma \quad , \; \mathcal{A}^{(S)}_{\Sigma^+ n\pi^+} \;=\; 0 \quad , \tag{25}$$

and $P-$wave amplitudes

$$\begin{aligned} \mathcal{A}^{(P)}_{\Lambda p\pi^-} \;&=\; \frac{g_A h_\Lambda}{M_\Lambda - M_n} + \frac{g_{\Lambda\Sigma} h_\Sigma}{M_p - M_{\Sigma^+}} \quad , \quad \mathcal{A}^{(P)}_{\Sigma^- n\pi^-} \;=\; \frac{g_{\Lambda\Sigma} h_\Lambda}{M_n - M_\Lambda} - \frac{g_{\Sigma\Sigma} h_\Sigma}{M_n - M_{\Sigma^0}} \;, \\ \mathcal{A}^{(P)}_{\Sigma^+ n\pi^+} \;&=\; \frac{g_{\Lambda\Sigma} h_\Lambda}{M_n - M_\Lambda} + \frac{g_{\Sigma\Sigma} h_\Sigma}{M_n - M_{\Sigma^0}} + \frac{g_A h_\Sigma}{M_{\Sigma^+} - M_p} \quad . \end{aligned} \tag{26}$$

We choose to fit the weak couplings $h_{\Lambda,\Sigma}$ to the central values of the $S-$wave amplitudes, and find that $h_\Lambda = 1.42$ and $h_\Sigma = 1.88$.

While the axial matrix elements $g_A = 1.27$ and $g_{\Lambda\Sigma} = 0.60$ are well-known experimentally, only an upper limit currently exists for $\Sigma^- \to \Sigma^0 e\overline{\nu}$, and thus there is no direct measurement of $g_{\Sigma\Sigma}$. Given the success of $SU(3)$ symmetry in relating the axial-current matrix elements, it is worth exploring its predictions for $g_{\Sigma\Sigma}$, along with the best estimates for leading-order $SU(3)$ breaking. In the limit of exact $SU(3)$, the axial-coupling would be $g_{\Sigma\Sigma} = F$, and thus $g_{\Sigma\Sigma} = 0.5$ at leading order. We focus on two quite different approaches to estimating the $SU(3)$ breaking. In one method [48], the one-loop corrections to all the axial matrix elements were computed in three-flavor χPT including the decuplet as dynamical fields, and parameters in the one-loop contributions were varied over a reasonable range in order to estimate the size of $SU(3)$ breaking effects. This analysis yields a range for $g_{\Sigma\Sigma}$, $0.35 \lesssim g_{\Sigma\Sigma} \lesssim 0.55$. However, the analysis is somewhat ad hoc and depends upon the convergence of the three-flavor chiral expansion, but formally captures the leading-order $SU(3)$ breaking in the chiral limit. The other method [52, 53] we use to estimate $g_{\Sigma\Sigma}$ is to perturb about the large$-N_C$ limit of QCD, a program that has been very successful in understanding known baryon properties, and has provided insight into the successes of the naive constituent quark model. This large$-N_C$ analysis of the axial matrix elements leads

to a range [11] $0.30 \lesssim g_{\Sigma\Sigma} \lesssim 0.36$ [12]. Given that these distinct estimates of $g_{\Sigma\Sigma}$ have only a small overlap and neither are obviously incorrect, we take $0.30 \lesssim g_{\Sigma\Sigma} \lesssim 0.55$ as the range of this axial coupling constant, and it is clear that it is quite uncertain at present.

Inserting numerical values for the couplings and masses into the $S-$wave and $P-$wave amplitudes in eq. (25) and eq. (26) gives the numerical values for the nonleptonic amplitudes shown in table II. At leading order, the $P-$wave amplitude in Λ decays is well predicted,

TABLE II: Weak Amplitudes in $SU(2)$ χPT at LO ($g_{\Sigma\Sigma} = 0.30 \to 0.55$)

Decay	$\mathcal{A}^{(S)}$ Theory	$\mathcal{A}^{(S)}$ Expt	$\mathcal{A}^{(P)}$ Theory	$\mathcal{A}^{(P)}$ Expt
$\Lambda \to p\pi^-$	1.42 (input)	1.42 ± 0.01	0.56	0.52 ± 0.02
$\Sigma^- \to n\pi^-$	1.88 (input)	1.88 ± 0.01	$-0.50 \to -0.14$	-0.06 ± 0.01
$\Sigma^+ \to n\pi^+$	0.0	0.06 ± 0.01	$+0.42 \to +0.08$	1.81 ± 0.01

as it is in the three-flavor theory. However, we do not expect significant modifications to this result from higher orders in the two-flavor theory. Further, we see that the $P-$wave amplitude for $\Sigma^- \to n\pi^-$ is quite sensitive to the value of $g_{\Sigma\Sigma}$, which is presently quite uncertain. At the upper limit of the allowed range for $g_{\Sigma\Sigma}$, the $P-$wave amplitude is close to what is observed. Finally, we see that the $P-$wave amplitude for $\Sigma^+ \to n\pi^+$ is not close to the experimental value for any reasonable value of $g_{\Sigma\Sigma}$, and theory underestimates the experimental value by ~ 4 in the best case.

[11] By extending the contents of table II in Ref. [53] the coupling $g_{\Sigma\Sigma}$ is found to be

$$g_{\Sigma\Sigma} \;=\; \frac{2}{3}a + b + \frac{4}{3}c_3 - \frac{2}{3}c_4 \quad . \tag{27}$$

Using the central values of the global fit values for the parameters a, b, c_3 and c_4 found in table VII of Ref. [53] we arrive at the range for $g_{\Sigma\Sigma}$. We thank Aneesh Manohar and Elizabeth Jenkins for assisting with this determination.

[12] For completeness we have also determined the axial coupling g_Ξ that appears in the interaction Lagrange density

$$\mathcal{L}_\pi \;=\; \frac{g_\Xi}{f}\,\overline{\Xi}\,\sigma\cdot\nabla M\,\Xi \;\;, \tag{28}$$

where Ξ denotes the iso-doublet containing the Ξ^0 and Ξ^-. By extending the contents of table II in Ref. [53] the coupling g_Ξ is found to be

$$g_\Xi \;=\; \left[\;\frac{1}{3}a - b + \frac{4}{3}c_3 - \frac{8}{3}c_4\;\right] \quad . \tag{29}$$

Using the central values of the global-fit values for the parameters a, b, c_3 and c_4 found in table VII of Ref. [53] we find $0.26 \lesssim g_\Xi \lesssim 0.30$. Further, the one-loop analysis of Ref. [48] gives $0.18 \lesssim g_\Xi \lesssim 0.36$. These two estimates are compatible with each other, with, as before, the estimate from Ref. [48] having a larger range than that from Ref. [53].

B. Nonleptonic Weak Decays of Hyperons and Lattice QCD

Given the failure of both $SU(2)$ and $SU(3)$ χPT to describe the $P-$wave amplitudes of the nonleptonic decays, one would like to understand where the problems lie. Until this issue is resolved, one is unable to claim theoretical control in the nonleptonic decays of hypernuclei. Lattice QCD is, of course, the only rigorous theoretical technique that exists to compute these decays, and it is important to use lattice simulations as a diagnostic of the problem(s) with the χPT calculations.

One should first compute the two-point functions that arise from the leading-order interactions in eq. (23). The lattice calculation of this process injects energy at the weak four-quark operator in order to allow both the initial and final states to be on mass-shell. Hence one must consider additional operators in the EFT that are usually discarded as surface terms. In the $SU(2)$ expansion, the mass difference between the Λ or Σ and the nucleon is taken to be a scale that is fixed in the chiral limit, with dependence on the quark masses arising at higher orders in the chiral expansion, i.e. the strange quark mass is fixed. One therefore has the free Lagrange density

$$\mathcal{L} \;=\; N^\dagger iv\cdot DN \;+\; \Lambda^\dagger iv\cdot\partial\Lambda \;-\; \Delta_{\Lambda N}\Lambda^\dagger\Lambda \;+\; \ldots \quad . \tag{30}$$

At NLO there are contributions from

$$\begin{aligned}\mathcal{L} \;=\; G_F m_{\pi^+}^2 \Big[\; j_\Lambda^{(1)}\; iv\cdot\partial\Big[\;\Big(\overline{N}h_\xi\Big)\,\Lambda\;\Big] \;+\; j_\Lambda^{(2)}\;\Delta_{\Lambda N}\Big(\overline{N}h_\xi\Big)\,\Lambda \\ +\; j_\Sigma^{(1)}\; iv\cdot\partial\Big[\;\overline{N}\Sigma h_\xi\;\Big] \;+\; j_\Sigma^{(2)}\;\Delta_{\Sigma N}\overline{N}\Sigma h_\xi \;+\; \text{h.c.}\;\Big] \quad ,\end{aligned} \tag{31}$$

where the surface terms vanish when energy and momentum are conserved at the effective weak vertex. However, in lattice calculations, where both the hyperon and the nucleon will be on mass-shell, these operators make a non-zero contribution to the amplitude at tree-level. This contribution must be included when attempting to extract the weak couplings $h_{\Lambda,\Sigma}$ from lattice calculations. Therefore, including such terms, the weak matrix element between a Λ and a nucleon arising from the diagrams shown in Fig. 5 becomes

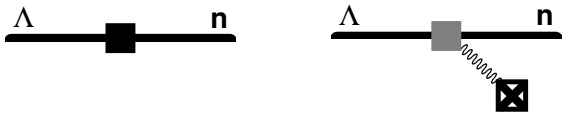

FIG. 5: *Tree-level diagrams that contribute to the weak $\Lambda \to N$ matrix element, including the leading-order surface term. The dark shaded square denotes an insertion of the weak vertex, h_Λ from eq. (23), while the light shaded square denotes an insertion of the weak vertices, $j_\Lambda^{(1,2)}$, from eq. (31). The crossed-square denotes an injection of energy at the weak vertex.*

$$\langle N\;(\mathbf{p}=0)|\;\mathcal{L}_{\text{weak}}\;|\Lambda\;(\mathbf{p}=0)\rangle \;=\; G_F m_{\pi^+}^2\Big[\;f\;h_\Lambda \;+\; \Delta_{\Lambda N}\;\Big(j_\Lambda^{(1)} \;+\; j_\Lambda^{(2)}\;\Big)\Big]\;\overline{U}_N U_\Lambda. \tag{32}$$

Given that the $P-$wave amplitude for $\Lambda \to p\pi^-$ is in good agreement with data, one expects that the value of h_Λ extracted from the lattice will be in agreement with that determined from the $S-$wave amplitudes. However, it is not clear what one will find for h_Σ

given the significant uncertainty in $g_{\Sigma\Sigma}$ and the complete failure to reproduce the $P-$wave amplitude for $\Sigma^+ \to n\pi^+$. Therefore, a lattice determination of h_Σ is highly desirable. Furthermore, given that there is a significant uncertainty in $g_{\Sigma\Sigma}$ and this uncertainty propagates through into a large uncertainty in the $P-$wave amplitudes for the Σ decays, a lattice determination of $g_{\Sigma\Sigma}$ is also highly desirable.

A direct lattice measurement of both the $S-$wave and $P-$wave amplitudes would also be very important. Assuming that the weak couplings $h_{\Lambda,\Sigma}$ and the axial couplings are all consistent with the above discussion, then we need to understand the origin of the failure of the $P-$wave amplitudes. Given the progress in extracting weak amplitudes for $K \to \pi\pi$ using the finite-volume techniques described by Lüscher and Lellouch [54] one can hope for a direct lattice determination of these amplitudes at some point in the future. While the actual value of the amplitude should agree with experiment one should be able to disentangle the various contributions to the amplitudes and understand where the failure originates in the low-energy EFT.

C. Weak Decays of Hypernuclei

A systematic study of the decays of hypernuclei provides an even greater challenge than describing the nonleptonic decays of hyperons in free-space. It will certainly be the case that the interactions that are ultimately needed to describe the nonleptonic decays will also provide a contribution, and likely a leading-order contribution, to the multi-baryon weak interactions such as $\Lambda N \to NN$. For instance, the diagram shown in Fig. 6 arises from

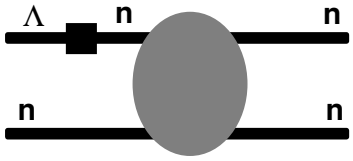

FIG. 6: *An example of a contribution to* $\Lambda n \to nn$.

inserting the weak two-point amplitude on an external leg of the strong $nn \to nn$ scattering amplitude. Unfortunately, there is presently no consistent EFT that is applicable in the kinematic regime for $\Lambda N \to NN$ where the energy release for an initial ΛN state at rest is $E \sim 176$ MeV. If an EFT exists for the strong processes, such as $\Lambda N \to \Lambda N$ and $NN \to NN$ at these relatively high energies, one hopes that the higher-dimension weak operators are subleading compared to the two-point function, but given the uncertainty in the nonleptonic hyperon decays and the absence of a strong-interaction EFT, it appears premature to make any such power-counting arguments at this stage.

However, having made all of these negative statements based on our current theoretical understanding, there has been an important phenomenological analysis [10, 11] recently completed by Parreño, Bennhold and Holstein (PBH) that gives one hope that an EFT can in fact be constructed to describe these processes. In PBH, contributions to the weak decay from weak-one-pion exchange (WOPE) and weak-one-kaon exchange (WOKE) were included

along with contributions from local $\Delta s = 1$ weak ΛNNN interactions. The power-counting used in determining the order of the various contributions is based on Weinberg's power-counting of NN interactions in which the number of powers of the small momenta is directly related to the order in the expansion. The weak interaction computed to a given order in Weinberg power-counting is then dressed with NN strong interactions in the final state and the initial-state interactions are taken into account by a correlated ΛN wavefunction determined from Nijmegen models.

The usual divergence problems with local four-baryon interactions arise in this calculation and are dealt with in PBH by extending the interaction in coordinate space to a Gaussian form with the same spatial integral (of course, the dependence upon the form of the regulator must be, and is, higher order in the power-counting). The results of a global fit, and data can be found in table III.

TABLE III: Weak decay observables for ${}^{5}_{\Lambda}$He, ${}^{11}_{\Lambda}$B and ${}^{12}_{\Lambda}$C taken from Ref. [10, 11]. The theoretical numbers correspond to including WOPE, WOKE along with the leading-order parity-violating and parity-conserving ΛNNN interactions with the short-distance parameters globally fit to the data.

Observable	Theory (best global fit) [10, 11]	Expt
$\Gamma({}^{5}_{\Lambda}\mathrm{He})$	0.44	0.41 ± 0.14 , 0.50 ± 0.07
n/p $({}^{5}_{\Lambda}\mathrm{He})$	0.55	0.93 ± 0.55 , 0.50 ± 0.10
$\mathcal{A}({}^{5}_{\Lambda}\mathrm{He})$	0.24	0.24 ± 0.22
$\Gamma({}^{11}_{\Lambda}\mathrm{B})$	0.88	0.95 ± 0.14
n/p $({}^{11}_{\Lambda}\mathrm{B})$	0.92	$1.04^{+0.59}_{-0.48}$
$\mathcal{A}({}^{11}_{\Lambda}\mathrm{B})$	0.09	-0.20 ± 0.10
$\Gamma({}^{12}_{\Lambda}\mathrm{C})$	0.93	1.14 ± 0.2 , 0.89 ± 0.15 , 0.83 ± 0.11
n/p $({}^{12}_{\Lambda}\mathrm{C})$	0.77	0.87 ± 0.23
$\mathcal{A}({}^{12}_{\Lambda}\mathrm{C})$	0.03	-0.01 ± 0.10

It is found that the overall goodness of the fit encapsulated in the χ^2 is independent of the range of the short-distance Gaussian regulator (over the range explored) and also independent of the strong-interaction potential used to compute the final-state interactions. This is very encouraging. The numerical values of the bare coefficients in the weak potential depend upon the range of the Gaussian regulator, as one would expect, but the dependence of the observables is minimal. Therefore, it appears that a systematic EFT description of the weak decays should be possible in the near future, and it may be as simple as Weinberg power-counting in many of the decay channels. Clearly, this exciting possibility requires further exploration.

It goes without saying that it would be very nice to see a calculation of the weak $\Lambda N \to NN$ amplitude directly from lattice QCD (a 5-point function!). While one knows how to extract the weak decay amplitudes for $K \to \pi\pi$ from the lattice, part of which is tuning the lattice volume so that one of the $\pi\pi$ energy states on the lattice is degenerate with a kaon at rest, no such formulation currently exists for extracting weak amplitudes for $2 \to 2$ processes. In principle we do not see any formal road blocks to constructing a framework analogous to that of Lüscher and Lellouch, however, given that the one-body decays are not yet understood we do not see any urgency in developing such a framework.

IV. CONCLUSIONS

We have explored some aspects of strong-interaction physics that impact our understanding of the structure and decays of hypernuclei and that could be addressed by lattice QCD simulations in the near future. In the few-nucleon sector, lattice QCD will provide an understanding of the strong dynamics, such as the fine-tuning that exists in the two-nucleon system, but it will not improve the precision of input into nuclear calculations of many-body observables. However, in the hypernuclear sector where experimental measurements are scarce and quite uncertain, lattice QCD may be in a position to compete with and ultimately surpass experiment and thus greatly aid progress in the field. We have discussed quantities in both the strong and weak sectors whose calculation in lattice QCD would have great significance.

To summarize, the lattice QCD calculations of strong-interaction processes that would be of fundamental importance for hypernuclear physics are:

- An extraction of the scattering length and effective range for ΛN scattering from finite-volume simulations;
- A determination of matrix elements of the axial current for $\Sigma \to \Sigma$, $g_{\Sigma\Sigma}$;
- A determination of the ηNN and $\eta\Lambda\Lambda$ hairpin couplings in PQQCD;

and of weak-interaction processes are:

- A measurement of the coefficients of the weak nonleptonic two-point functions, h_Λ and h_Σ;
- A measurement of both the $S-$ and $P-$wave amplitudes for the weak nonleptonic decays, e.g. $\Lambda \to p\pi$;
- A measurement of the amplitude for the weak scattering $\Lambda N \to NN$.

A lattice QCD determination of any one of these quantities would significantly improve our understanding of hyperons, and hypernuclei in general.

Acknowledgments

We would like to thank Will Detmold, Elizabeth Jenkins, David Lin and Aneesh Manohar for helpful discussions and SRB, AP and MJS would like to thank Paulo Bedaque for organizing the *Effective Summer in Berkeley* workshop at LBL this past summer where this work was initiated. We also thank Rob Timmermans for a very-detailed analysis and discussion of the scattering parameters for hyperon-nucleon scattering. The work of SRB was partly supported by DOE contract DE-AC05-84ER40150, under which the Southeastern Universities Research Association (SURA) operates the Thomas Jefferson National Accelerator Facility. PFB was supported by the Director, Office of Energy Research, Office of High Energy and Nuclear Physics, and by the Office of Basic Energy Sciences, Division of Nuclear Sciences, of the U.S. Department of Energy under Contract No. DE-AC03-76SF00098. MJS is supported in part by the U.S. Dept. of Energy under Grant No. DE-FG03-97ER4014. AP is supported by the MCyT under Grant No. DGICYT BFM2002–01868 and by the Generalitat de Catalunya under Grant No. SGR2001–64.

V. APPENDIX I : LÜSCHER'S RELATIONS FROM EFT($\not\pi$)

From the discussions in Refs. [22, 23] it is clear that in the pionless theory describing non-relativistic baryons, each of mass M, the exact two-body elastic scattering amplitude in the continuum is

$$\mathcal{A} \;=\; \frac{\sum C_{2n} p^{2n}}{1 - I_0 \sum C_{2n} p^{2n}} \quad , \quad I_0 \;=\; \left(\frac{\mu}{2}\right)^{4-D} \int \frac{d^{D-1}\mathbf{q}}{(2\pi)^{D-1}} \frac{1}{E - \frac{|\mathbf{q}|^2}{M} + i\epsilon} \quad , \tag{33}$$

where the C_{2n} are the coefficients of operators with $2n$ derivatives acting on the nucleon fields (or equivalently with n time derivatives). Applying the PDS scheme to I_0 gives

$$I_0^{(PDS)} \;=\; -\frac{M}{4\pi}\;(\mu + ip) \;+\; \mathcal{O}(D-4) \quad , \tag{34}$$

where $p = \sqrt{ME}$ and hence

$$\mathcal{A} \;=\; \frac{4\pi}{M}\;\frac{1}{p\cot\delta - ip} \quad , \tag{35}$$

where the subtraction-scale dependence of the one-loop diagrams is exactly compensated by the corresponding dependence of the coefficients $C_{2n}(\mu)$. δ is the energy-dependent $S-$wave phase shift (we will only consider $S-$wave scattering but this construction generalizes to all partial waves).

We are interested in the energy-eigenvalues of this system placed in a box with sides of length L with periodic boundary conditions. We can find the energy-eigenvalues by requiring that the real part of the inverse scattering amplitude computed in the box vanishes,

$$\frac{1}{\sum C_{2n}(\mu)\; p^{2n}} \;-\; \mathrm{Re}(I_0^{(PDS)}(L)) \;=\; 0 \quad , \tag{36}$$

where

$$I_0(L) \;=\; \frac{1}{L^3}\sum_{\mathbf{k}} \frac{1}{E - \frac{|\mathbf{k}|^2}{M}} \quad , \tag{37}$$

and the sum is over momenta, $\mathbf{k}$, allowed on the lattice.

The PDS value of this linearly-divergent integral is found by adding and subtracting the continuum limit of the integral evaluated at $E = 0$. One of the continuum integrals is evaluated with a momentum cut-off that is equal to the mode cut-off of the discrete summation, while the other is evaluated with dimensional-regularization and PDS. The subtraction-scheme dependence vanishes as expected, and we find that eq. (36) becomes

$$p\cot\delta(p) \;-\; \frac{1}{\pi L}\sum_{\mathbf{j}}^{\Lambda_j} \frac{1}{|\mathbf{j}|^2 - (\frac{Lp}{2\pi})^2} \;+\; \frac{4\Lambda_j}{L} \;=\; 0 \quad , \tag{38}$$

where the limit $\Lambda_j \to \infty$ is understood, and where Λ_j is the magnitude of the integer cut-off, related to the momentum cut-off in the box defined via $|\mathbf{k}_{\mathrm{max.}}| = 2\pi\Lambda_j/L$. Solving for the values of p for which eq. (38) is satisfied recovers Lüschers result(s) [27, 28]. Given that Λ_j is set by the edge of the first Brillouin zone, clearly one must not be too cavalier about

taking the $\Lambda_j \to \infty$ limit in present day calculations [13], however, in this work we will take the limit $\Lambda_j \to \infty$. This derivation of Lüscher's formula [27, 28] makes explicit the analytic continuation of the zeta-functions that appear in his expressions.

Using the effective-range expansion of $p \cot \delta$

$$p \cot \delta \;=\; -\frac{1}{a} \;+\; \frac{1}{2} r p^2 \;+\; \ldots \quad , \tag{39}$$

and assuming that $L \gg a, r$ [14] one finds that the lowest-energy eigenvalue is

$$E_0 \;=\; +\frac{4\pi a}{M L^3} \left[\; 1 \;-\; c_1 \frac{a}{L} \;+\; c_2 \left(\frac{a}{L} \right)^2 \;+\; \ldots \right] \;+\; \mathcal{O}(L^{-6}) \quad , \tag{40}$$

where the coefficients $c_{1,2}$ are

$$\begin{aligned} c_1 \;&=\; \frac{1}{\pi} \left(\sum_{\mathbf{j} \neq 0}^{\Lambda_j} \frac{1}{|\mathbf{j}|^2} - 4\pi\Lambda_j \right) \;=\; -2.837297 \;=\; \frac{1}{\pi} Z_{00}(1,0) \; ; \\ c_2 \;&=\; c_1^2 - \frac{1}{\pi^2} \sum_{\mathbf{j} \neq \mathbf{0}} \frac{1}{|\mathbf{j}|^4} \;=\; 6.375183 \;=\; \frac{1}{\pi^2} \Big(\; (Z_{00}(1,0))^2 - Z_{00}(2,0) \; \Big) \quad , \end{aligned} \tag{41}$$

where the $Z_{00}(n,k)$ are defined in Refs. [27, 28],

$$Z_{00}(n,k) \;=\; \lim_{\Lambda_j \to \infty} \left(\sum_{\mathbf{j}, |\mathbf{j}| \neq k}^{\Lambda_j} \frac{1}{(|\mathbf{j}|^2 - k^2)^n} \;-\; \delta^{n1} \; 4\pi\Lambda_j \right) \quad , \tag{42}$$

for integers $n \geq 1$ and k. It is important to note that there are sign differences between our result in eq. (40) and the analogous expression in Ref. [27, 28]. This is due to the opposite sign convention for the scattering length a, for which we use that common to nuclear physicists.

We also need the energy of the next state in order to extract both the scattering length and the effective range. The construction is somewhat more complicated than that for the lowest state. One looks at the energy of the next-most energetic level that is invariant under the action of the complete cubic group; the space of such states is the A_1 sector [27, 28]. It is easy to show from the decomposition of the full rotation group down to the cubic group [56] that the energy shift of such states due to the two-body interaction receives contributions from $l = 0, 4, 6, ..$ interactions, where l is the angular momentum of the interaction. Therefore, to the order we are working in the momentum expansion, the shift in the energy-levels is sensitive to $S-$wave interactions only. It is straightforward to show that the energy of the next-highest state in the A_1 representation of the cubic group is [27, 28]

$$E_1 \;=\; \frac{4\pi^2}{M L^2} - \frac{12 \tan \delta_0}{M L^2} \Big(\; 1 + c_1' \tan \delta_0 + c_2' \tan^2 \delta_0 \;+\; \ldots \; \Big) \;+\; \mathcal{O}(L^{-6}) \; ;$$

[13] This issue is discussed in Ref. [55]. We thank William Detmold and David Lin for discussions regarding this point.

[14] It is interesting to note that one can also use this expression to find the energy-eigenvalues in the limit where $r \ll L \ll a$, as may be appropriate for two- or few-body nuclear physics observables. We will explore this limit in forthcoming work.

$$
\begin{aligned}
c_1' &= \frac{1}{2\pi^2} Z_{00}(1,1) \ ; \\
&= \frac{1}{2\pi^2}\left[\pi c_1 + \pi^2 c_1^2 - \pi^2 c_2 - 13 + \sum_{\mathbf{j},|\mathbf{j}|\neq 0,1}^{\Lambda_j} \frac{1}{|\mathbf{j}|^4(|\mathbf{j}|^2-1)} \right] \ = \ -0.061367 \ ; \\
c_2' &= \frac{1}{4\pi^4}\left(\ (Z_{00}(1,1))^2 - 6 Z_{00}(2,1) \ \right) \ ; \\
&= c_1'^2 + \frac{3}{2\pi^4}\left(\ \pi^2 c_2 - \pi^2 c_1^2 + 5 - \sum_{\mathbf{j},|\mathbf{j}|\neq 0,1}^{\Lambda_j} \frac{2|\mathbf{j}|^2-1}{|\mathbf{j}|^4(|\mathbf{j}|^2-1)^2} \ \right) \ = \ -0.354156 \quad , \qquad (43)
\end{aligned}
$$

where δ_0 is the $S-$wave phase shift evaluated at the unperturbed lattice momentum, $|\mathbf{p}| = 2\pi/L$, and coefficients $c_{1,2}'$ are those found by Lüscher [27, 28]. We have given expressions for $c_{1,2}'$ in terms of $c_{1,2}$ that can be straightforwardly evaluated and converge rapidly.

To generalize the expressions in eq. (40) and eq. (43) to ΛN scattering we make the replacement $M \to 2\mu_{\Lambda N}$ and understand that δ_0 is the phase shift for ΛN scattering with the scattering lengths and effective ranges discussed in the text evaluated at the unperturbed momentum $|\mathbf{p}| = 2\pi/L$.

---

[1] For a review and comparative study of the different reaction mechanisms, see W. Alberico and G. Garbarino, *Phys. Rept.* **369**, 1 (2002), `nucl-th/0112036`.

[2] J.J. Szymanski *et al.*, *Phys. Rev.* **C43**, 849 (1991); H. Noumi *et al.*, *Phys. Rev.* **C52**, 2936 (1995); H. Outa *et al.*, talk presented at the VIIIth Intl. Conf. on Hypernuclear and Strange Particle Physics (HYP03), Jefferson Lab, Newport News, Virginia, Oct. 14-18, 2003, To be published in *Nucl. Phys.* **A**.

[3] J. Golak, K. Miyagawa, H. Kamada, H. Witala, W. Glöckle, A. Parreño, A. Ramos, and C. Bennhold, *Phys. Rev.* **C55**, 2196 (1997); *ibid. Phys. Rev.* **C56**, 2892 (1997).

[4] A. Nogga, H. Kamada, and W. Glöckle, *Phys. Rev. Lett.* **88**, 172501 (2002), `nucl-th/0112060`.

[5] E. Hiyama, Y. Kino, M. Kamimura, *Prog. Part. Nucl. Phys.* **51**, 223 (2003).

[6] C.L. Korpa, A.E.L. Dieperink and R.G.E. Timmermans, *Phys. Rev.* **C65**, 015208 (2001), `nucl-th/0109072`.

[7] J.F. Dubach, G.B. Feldman and B.R. Holstein, *Annals Phys.* **249**, 146 (1996), `nucl-th/9606003`.

[8] A. Parreño, A. Ramos, and C. Bennhold, *Phys. Rev.* **C56**, 339 (1997),`nucl-th/9611030`; A. Parreño and A. Ramos, *Phys. Rev.* **C65** (2002) 015204,`nucl-th/0104080`.

[9] T. Inoue, K. Sasaki, M. Oka, *Nucl. Phys.* **A670**, 301 (2000).

[10] A. Parreño, C. Bennhold and B.R. Holstein, `nucl-th/0308074`.

[11] A. Parreño, C. Bennhold and B.R. Holstein, `nucl-th/0308056`.

[12] M. Fukugita, Y. Kuramashi, M. Okawa, H. Mino and A. Ukawa, *Phys. Rev. Lett.* **73**, 2176 (1994), `hep-lat/9407012`; *Phys. Rev.* **D52**, 3003 (1995), `hep-lat/9501024`.

[13] `http://nn-online.sci.kun.nl/index.html`.

[14] B. Sechi-Zorn, B. Kehoe, J. Twitty and R.A. Burnstein, *Phys. Rev.* **175**, 1735 (1968).

[15] G. Alexander, U. Karshon, A. Shapira, G. Yekutieli, R. Engelmann, H. Filthuth and W. Lughofer, *Phys. Rev.* **173**, 1452 (1968).

[16] See, for instance, Y.C. Tang, in *Proc. of the Int. Conf. on Hypernuclear Physics*, Argonne Nat.

Lab. (Ed. A.R. Bodmer and L.G. Hyman), p. 276; R.C. Herndon and Y.C. Tang, *Phys. Rev.* **159**, 835 (1967); R.H. Dalitz, R.C. Herndon and Y.C. Tang, *Nucl. Phys.* **B47**, 109 (1972); T.H. Tan, *Phys. Rev. Lett.* **23**, 395 (1969); J.J. de Swart *et al.*, *Springer Tracts in Modern Physics* **60**, 138 (1971).
[17] S. Weinberg, *Phys. Lett.* **B251**, 288 (1990).
[18] S. Weinberg, *Nucl. Phys.* **B363**, 3 (1991).
[19] C. Ordonez and U. van Kolck, *Phys. Lett.* **B291**, 459 (1992).
[20] C. Ordonez, L. Ray and U. van Kolck, *Phys. Rev. Lett.* **72**, 1982 (1994).
[21] D.B. Kaplan, M.J. Savage and M.B. Wise, *Nucl. Phys.* **B478**, 629 (1996), nucl-th/9605002.
[22] D.B. Kaplan, M.J. Savage and M.B. Wise, *Phys. Lett.* **B424**, 390 (1998), nucl-th/9801034.
[23] D.B. Kaplan, M.J. Savage and M.B. Wise, *Nucl. Phys.* **B534**, 329 (1998), nucl-th/9802075.
[24] D.B. Kaplan, M.J. Savage and M.B. Wise, *Phys. Rev.* **C59**, 617 (1999), nucl-th/9804032.
[25] S.R. Beane, P.F. Bedaque, M.J. Savage and U. van Kolck, *Nucl. Phys.* **A700**, 377 (2002), nucl-th/0104030.
[26] M.C. Birse, J.A. McGovern and K.G. Richardson, *Phys. Lett.* **B464**, 169 (1999), hep-ph/9807302.
[27] M. Lüscher, *Commun. Math. Phys.* **105** 153 (1986).
[28] M. Lüscher, *Nucl. Phys.* **B354**, 531 (1991).
[29] H.W. Hammer, *Nucl. Phys.* **A705**, 173 (2002), nucl-th/0110031.
[30] J.W. Chen and M.J. Savage, *Phys. Rev.* **D65**, 094001 (2002), hep-lat/0111050.
[31] S.R. Beane and M.J. Savage, *Nucl. Phys.* **A709**, 319 (2002), hep-lat/0203003.
[32] S.R. Beane and M.J. Savage, *Nucl. Phys.* **B636**, 291 (2002), hep-lat/0203028.
[33] S.R. Beane and M.J. Savage, *Phys. Lett.* **B535**, 177 (2002), hep-lat/0202013.
[34] S.R. Beane and M.J. Savage, *Phys. Rev.* **D67**, 054502 (2003), hep-lat/0210046.
[35] D. Arndt, S.R. Beane and M.J. Savage, *Nucl. Phys.* **A726**, 339 (2003), nucl-th/0304004.
[36] P.L. Cho, *Nucl. Phys.* **B396**, 183 (1993); [Erratum-ibid. **B421**, 683 (1994)], hep-ph/9208244.
[37] R.F. Dashen, E. Jenkins and A.V. Manohar, *Phys. Rev.* **D49**, 4713 (1994), [Erratum-ibid. **D51**, 2489 (1995)], hep-ph/9310379.
[38] D.B. Kaplan and M.J. Savage, *Phys. Lett.* **B365**, 244 (1996), hep-ph/9509371.
[39] S.R. Sharpe and N. Shoresh, *Phys. Rev.* **D64**, 114510 (2001), hep-lat/0108003.
[40] L. Maiani and M. Testa, *Phys. Lett.* **B245**, 585 (1990).
[41] K. Huang and C.N. Yang, *Phys. Rev.* **105**, 767 (1957).
[42] J.W. Chen, G. Rupak and M.J. Savage, *Nucl. Phys.* **A653**, 386 (1999), nucl-th/9902056.
[43] U. van Kolck, *Nucl. Phys.* **A645**, 273 (1999), nucl-th/9808007.
[44] P. van Baal, In the Boris Ioffe Festschrift, *At the frontier of particle physics*, vol. 2, 683-760, ed. by M. Shifman, World Scientific, hep-ph/0008206.
[45] J.F. Donoghue, E. Golowich and B.R. Holstein, *Cambridge Monogr. Part. Phys. Nucl. Phys. Cosmol.* **2**, 1 (1992).
[46] E. Jenkins, *Nucl. Phys.* **B375**, 561 (1992).
[47] E. Jenkins and A.V. Manohar, UCSD-PTH-91-30, *Talk presented at the Workshop on Effective Field Theories of the Standard Model, Dobogoko, Hungary, Aug 1991.*
[48] M.J. Savage and J. Walden, *Phys. Rev.* **D55**, 5376 (1997), hep-ph/9611210.
[49] R.P. Springer, hep-ph/9508324.
[50] R.P. Springer, *Phys. Lett.* **B461** (1999) 167.
[51] A. Abd El-Hady and J. Tandean, *Phys. Rev.* **D61**, 114014 (2000), hep-ph/9908498.
[52] J. Dai, R.F. Dashen, E. Jenkins and A.V. Manohar, *Phys. Rev.* **D53**, 273 (1996),

hep-ph/9506273.
[53] R. Flores-Mendieta, E. Jenkins and A.V. Manohar, *Phys. Rev.* **D58**, 094028 (1998), hep-ph/9805416.
[54] L. Lellouch and M. Lüscher, *Commun. Math. Phys.* **219**, 31 (2001), hep-lat/0003023.
[55] C.J. Lin, G. Martinelli, C.T. Sachrajda and M. Testa, *Nucl. Phys.* **B619**, 467 (2001), hep-lat/0104006.
[56] J.E. Mandula, G. Zweig and J. Govaerts, *Nucl. Phys.* **B228**, 91 (1983).